The global clonal complexity of the murine blood system declines throughout life and after serial transplantation

Miguel Ganuza[1], Trent Hall[1], David Finkelstein[3], Yong-Dong Wang[3], Ashley Chabot[1], Guolian Kang[2], Wenjian Bi[2], Gang Wu[3] and Shannon McKinney-Freeman[§1].

[1]Department of Hematology, [2]Department of Biostatistics and [3]Department of Computational Biology, St. Jude Children's Research Hospital, Memphis, TN, 38105

Text word count: Main text (Introduction, Methods, Results and Discussion; 4631 words), Abstract (200 words), 7 Figures, 6 Supplemental Figures, one Table, three Supplemental Tables and 93 references.

Short title (48 characters including spaces): The clonal complexity of blood declines with age

§ Corresponding author

Key points

1) **The clonal diversity of the hematopoietic system declines with age and after serial transplantation.**

2) **Aged HSC acquire mutations that might confer a selective advantage during serial transplantation**

Abstract (limit: 200 words; Current: 200 words)

Although many recent studies describe the emergence and prevalence of 'clonal-hematopoiesis of indeterminate-potential' (CHIP) in aged human populations, a systematic analysis of the numbers of clones supporting steady-state hematopoiesis throughout mammalian life is lacking. Previous efforts relied on transplantation of 'barcoded' hematopoietic stem cells (HSC) to track the contribution of HSC clones to reconstituted blood. However, *ex vivo* manipulation and transplantation alter HSC function and thus may not reflect the biology of steady-state hematopoiesis. Using a non-invasive *in vivo* color-labeling system, we report the first comprehensive analysis of the changing global clonal complexity of steady-state hematopoiesis during the natural murine lifespan. We observed that the number of clones (*i.e.* clonal complexity) supporting the major blood and bone marrow hematopoietic compartments decline with age by about 30% and 60%, respectively. Aging dramatically reduced HSC *in vivo* repopulating activity and lymphoid potential while increasing functional heterogeneity. Continuous challenge of the hematopoietic system by serial transplantation provoked the clonal collapse of both young and aged hematopoietic systems. Whole exome sequencing of serially transplanted aged and young hematopoietic clones confirmed oligoclonal hematopoiesis and revealed mutations in at least 27 genes, including nonsense, missense and deletion mutations in *Bcl11b, Hist1h2ac, Npy2r, Notch3, Ptprr* and *Top2b*.

56

Introduction

Advances in technology and medicine have freed modern *Homo sapiens* from natural selection imposed by the environment, predation and disease, increasing the incidence of aging pathologies[1]. Genomic instability, telomere attrition, epigenetic alterations and perturbed proteostasis contribute to disrupted tissue homeostasis (*i.e.* stem cell exhaustion) in the aged[2]. Aged blood displays a loss of adaptive immunity and higher incidences of anemia and myeloid malignancies[3]. Additionally, expanded hematopoietic clones are apparent in the peripheral blood (PB) of many aged individuals[4-13]. >70% of humans older than 90 years display CHIP (defined as ≥2%PB from a single cellular clone)[4-11]. *DNMT3A, TET2, ASXL1, PPM1D* and *JAK2* are often mutated in CHIP patients[6,7], who have a three- and 11-fold greater risk of developing cardiovascular diseases or leukemia, respectively[6,11,14].

Unknown is how many cellular clones actively contribute to hematopoiesis throughout life and how these numbers change with age[8]. Previous studies interrogating clonal behavior in aged mammalian blood utilized HSC transplantation or mathematical modeling[15,16,17]. Transplantation imposes tremendous stress on HSC[18]. Thus, studies based entirely on transplantation and *ex vivo* manipulation of HSC may not accurately reflect steady-state hematopoiesis[19-21]. Understanding the dynamics of the clonal complexity of blood throughout life requires non-invasive strategies. We recently reported a new approach to study the endogenous clonal complexity of blood that takes advantage of a *Cre recombinase* (CRE) inducible multi-color allele (*i.e. Confetti* allele)[22,23]. Here, employing this approach and multiple CRE labeling strategies, we

observed a loss of clonal complexity in all hematopoietic compartments with age during steady-state hematopoiesis. Further, repeated exposure to extreme hematopoietic stress by serial transplantation resulted in the clonal collapse of both aged and young blood. Whole exome sequencing (WES) of serially transplanted bone marrow (BM) confirmed oligoclonal hematopoiesis and identified mutations in aged hematopoietic clones in genes not previously implicated in HSC self-renewal and maintenance (*e.g. Bcl11b, Hist1h2ac, Npy2r, Notch3, Ptprr*, *Top2b*). These mutations might be important for HSC clonal expansion during aging and hematopoietic stress.

Methods

Mice

C57BL/6J, C57BL/6.SJL-PtprcaPep3b/BoyJ, *Flk1*$^{+/Cre}$ (Flk1Kdr$^{tm1(cre)Sato/J}$), *ROSA26*$^{+/Confetti}$ (Gt(ROSA)26Sor$^{tm1(CAG-Brainbow2.1)Cle/J}$) and *E2a*$^{+/Cre}$ (B6.FVB-Tg(EIIa-cre)C5379Lmgd/J) (Jackson Laboratory, Bar Harbor, Maine) mice were housed in a pathogen-free facility. All animal experiments were carried out according to procedures approved by the St. Jude Children's Research Hospital Institutional Animal Care and Use Committee.

Genotyping

Genotyping of *Cre* and *Confetti* alleles was as previously described[23].

Transplants

0.2x10^6, 1x10^6 or 5x10^6 whole BM cells from young (age two months), old (age 24-26 months) CD45.2$^+$ *ROSA26*$^{+/Confetti}$*VE-Cadherin*$^{+/Cre}$ mice or from primary, secondary or tertiary recipient mice were transplanted via tail vein into 8-12 week old CD45.2$^+$/CD45.1$^+$ C57BL/6J mice previously subjected to 11 Gy of ionizing radiation in split doses of 5.5 Gy.

Cell division kinetics

Single HSCs sorted into 96-well plates were inspected to follow division kinetics every 12 hours for 72 hours as described[24]. Details in Supplemental Materials and Methods.

Differentiation potential assay

Single HSCs were sorted into 96-well plates and cultured in myeloid differentiation medium for 14 days as described[25]. Emerging colonies were harvested, stained and analyzed for myeloid lineages. Details in Supplemental Materials and Methods.

PB Analysis

PB was collected, stained and analyzed as described[23].

Bone Marrow Analysis

BM was harvested from the femurs, tibias, and pelvic bones of mice by crushing. c-Kit$^+$ cells were enriched using anti-c-Kit microbeads (Miltenyi Biotech, San Diego, CA) followed by magnetic separation (autoMACS Pro Separator; Miltenyi Biotech). Cells were stained with antibodies to HSC, MPPs, CMPs, GMPs, MEPs and CLPs. Details in Supplemental Materials and Methods.

Statistics and use of formula for predicting cell number from sample-to-sample variance

Summary statistics, including mean, median, minimum, maximum, percentile 25, percentile 75 and standard deviation were reported. To calculate the clonal complexity of any tissue at any given time point, we used the mouse-to-mouse variance in *Confetti* color distribution[23]. Detailed in Supplemental Materials and Methods.

WES-Sample collection, preparation and analysis

Genomic DNA was isolated using Quick-DNA™ Miniprep Kit (Catalog No. D3024; Zymo Research, Irvine, CA). Genomic libraries were generated using SureSelectXT kit specific for the Illumina HiSeq instrument (Catalog No. G9611B; Agilent Technologies, Santa Clara, CA), followed by exome enrichment (SureSelect XT Mouse All Exon bait set; Catalog No. 5190-4642). Exome enriched libraries were then sequenced by the St. Jude Genome Sequencing Facility.

To identify somatic mutations within each transplant group, whole-exome-sequences of CD45.1$^-$ *Confetti* clones isolated from the same donor group were compared to each other and to CD45.1$^-$ *Confetti* clones isolated from distinct donor groups. Details in Supplemental Materials and Methods.

Data sharing statement

For original data please contact shannon.mckinney-freeman@stjude.org.

Results

The clonal complexity of native hematopoiesis declines with age

To illuminate the clonal dynamics of native hematopoiesis throughout life, we genetically labeled the hematopoietic system of mouse cohorts during embryonic development and analyzed the subsequent evolution of global clonal complexity. Specifically, we examined the mouse-to-mouse variance (MtMV) in *Confetti* color distribution in the blood and c-Kit$^+$ BM of cohorts of *ROSA26*$^{+/Confetti}$*E2a*$^{+/Cre}$ mice (*Conf-E2a*^{Cre}), *ROSA26*$^{+/Confetti}$*Flk-1*$^{+/Cre}$ (*Conf-Flk-1*^{Cre}), *ROSA26*$^{+/Confetti}$*VE-Cadherin*$^{+/Cre}$ mice (*Conf-VE*^{Cre}), and *ROSA26*$^{+/Confetti}$*Vav1*$^{+/Cre}$ mice (*Conf-Vav1*^{Cre}) from two to 26 months of age (Figure 1A). The *Confetti* reporter allele is recombined by CRE and randomly labels progeny with GFP, YFP, RFP or CFP (Supplemental Figures 1A-B). Here, *Confetti* labeling is initiated in blastomeres (*Conf-E2a*^{Cre}), mesodermal hematopoietic precursors (*Conf-Flk-1*^{Cre}), hemogenic endothelial precursors (*Conf-VE*^{Cre}) and definitive hematopoietic stem and progenitor cells (HSPCs) (*Conf-Vav1*^{Cre}) (Figure 1A). As previously established, large numbers of *Confetti*+ precursors contributing to a given cell population results in a small MtMV of *Confetti* colors while small numbers of *Confetti*+ precursors results in high MtMV of *Confetti* colors (Figure 1B)[23]. The following formula estimates the number of contributing clones using the observed MtMV in *Confetti* colors: Cell number = $10^{(-1.56 \times \log10(CV)+1.47)}$(where CV= standard deviation/mean and represents the coefficient of variance). This formula yields accurate estimates of numbers of contributing clones when that number falls between 50 and 2500 clones[23]. For *Conf-Flk-1*^{Cre}, *Conf-VE*^{Cre} and *Conf-Vav1*^{Cre} mice, PB clonal complexity at two months fell within this range (about 600, Figure 1Ci). As expected, PB and BM clonal complexity of *Conf-*

179 *E2a*^{Cre} mice fell below this range, as these mice express CRE when embryos are
180 comprised of very few cells. It therefore serves as a control for low complexity (Figure
181 1A-Ci). Thus, about 600 cells labeled during embryonic development represent the
182 precursors for the entire HSC pool in young adult mice (about 20,000 HSC)[26-30]. This
183 number serves as an initial benchmark from which we grossly examined how relative
184 clonal complexity of blood changes with time. Across CRE lines, PB clonal complexity
185 was stable until 16-20 months of age, after which it steadily declined for all cohorts
186 except *Conf-E2a*^{Cre} (Figure 1Ci-Cii, Supplemental Figure 1D). Clonal complexity
187 dropped slightly earlier in myeloid cells (Supplemental Figure 1D). On average, we
188 observed a 24% drop in PB clonal complexity of aged mice at 24 and 26 months relative
189 to young mice (p-value=0.03 and 0.01; FDR q-value(q)=0.1 and 0.06, respectively)
190 (Figure 1Cii). At 24 months, PB clonal complexity was reduced an average of 11.1%,
191 37.2% and 44.0% in B cell, T cell and myeloid cell lineages, respectively (Supplemental
192 Figure 1D).
193
194 Most BM HSPC compartments displayed a drop in overall clonal complexity with age in
195 *Conf-Flk-1*^{Cre}, *Conf-VE*^{Cre} and *Conf-Vav1*^{Cre} mice strains (Figure 1Di). On average, the
196 clonal complexity of HSC and MPP in aged mice decreased by 59.3% (p=0.045,
197 q=0.1578) and 69.6% (p=0.053, q=0.1578), respectively (Figure 1Dii). While CLP, CMP
198 and GMP displayed about a 65.6% (p=0.232), 32.3% (p=0.229) and 42.7% (p=0.0964,
199 q=0.1928) clonal loss, MEP only lost 44.2% (p=0.383) of clonal complexity with age
200 (Figure 1Dii). As expected, *Conf-E2a*^{Cre} mice showed no loss of BM complexity (Figure
201 1Di). Altogether, these data reveal a global loss of clonal complexity with age in all BM

compartments labeled after the blastomere stage. Interestingly, HSC and MPP were more sensitive to the selective pressures imposed by aging than other HSPC.

Native hematopoiesis is characterized by clonal instability

Our study and others suggest that native hematopoiesis is polyclonal[19,20]. The behavior of individual HSC clones over time can be explained by clonal succession (distinct clones progressively recruited)[31-33], clonal stability (same clones steadily contributing)[15,34], dynamic repetition (a specific clone recruited multiple times)[35] or a combination of these models[36]. Although our system cannot track individual clones, it can follow "pooled-clones", which are clones labeled with the same *Confetti* color. GFP-labeled pools are particularly useful because *Confetti*-allele driven GFP labeling is under-favored in most tissues[22,23,37]. Thus, GFP+ hematopoietic cells almost certainly reflect the activity of a smaller pool of clones than RFP, CFP or YFP and are useful for tracking the dynamics of a relatively small number of clones.

Here, we analyzed in individual mice the evolution of GFP-labeled clonal pools. Aging was occasionally accompanied by dramatic changes in PB GFP-labeling (Figure 2, Supplemental Figure 2). For example, we observed expansions of GFP-pooled-clones with age (*e.g. Conf-E2a*^{Cre} Mouse #1 and *Conf-VE*$^{/Cre}$ Mouse #1, Figure 2A). Both expansion and constriction of GFP-pooled-clones (*e.g. Conf-Flk1*^{Cre} Mouse #3, *Conf-Vav1*^{Cre} Mouse #3, Figure 2A) and YFP-pooled-clones were also detected (*e.g. Conf-E2a*^{Cre} Mouse #3, Figure 2A). The relative change in the PB frequency of GFP from time-point to time-point throughout the life of individual mice revealed this as a common

phenomenon observed across PB lineages (Figure 2B, Supplemental Figure 2). These data support a model of PB clonal instability, in which clonal pools wax and wane throughout life.

Aging increases the functional heterogeneity of the HSC pool

HSCs give rise to downstream BM progenitors [21]. To gain insight into the functional consequences of aging on HSC, the division kinetics and differentiation potential of single young and aged HSC was examined. Aged HSCs displayed slower division kinetics than young HSCs (Figure 3A). Aging also decreased the frequency of multi-potent HSC (Figure 3B, Supplemental Figure 3). These data suggest an increase in HSC functional heterogeneity with age.

To address this *in vivo*, we again examined the behavior of 'pooled' clones labeled with the same *Confetti* color. A similar distribution of *Confetti* colors among distinct BM compartments in individuals reflects a close lineage relationship. For example, when one examines the BM of *Conf-E2a*^{Cre} Mouse #6 or *Conf-Vav*^{Cre} Mouse #5 at 26 months, HSC and MPP displayed a similar distribution of *Confetti* colors relative to downstream HSPC (Figure 3B). To globally analyze these patterns, we calculated the correlation (Pearson's correlation coefficient) in the percent contribution of each *Confetti* color to different cell lineages in young and old mice (Figure 3C). The correlation between lineages declined with age (see color intensity in Figures 3Ci-ii). Remarkably, the correlation between HSC and MPP was less eroded with age compared to the correlation of HSC with other HSPC (Figure 3Ciii). Additionally, the pattern of correlation among different lineages in young

mice was similar in aged mice (see the color pattern in Figures 3Cii and Supplemental Figure 3B where the scale is modified in young mice to facilitate comparison). These data suggest that HSC continuously produce MPP throughout life and aging increases the functional heterogeneity of the HSC pool, which is reflected in the eroded correlations between HSC and other BM compartments (p-value=0.03).

Aging constrains HSC repopulating activity

To further investigate the effect of aging on HSC self-renewal and function, we repeatedly challenged aged HSC by serially transplanting *Conf-VE*^{Cre}-BM into irradiated recipients (Figure 4, Supplemental Figure 4). Here, BM from three independent young and aged donors was independently serially transplanted into a total of six cohorts of mice: young BM (groups A-C) and aged BM (groups D-F) (Figures 5-6, Supplemental Figure 5). Thus, all *Confetti*+ BM within each group ultimately derives from the same primary donor.

Our *Confetti*-based approach faithfully estimates PB repopulating units (RUs) at short and long-time points post-transplant[23]. In primary transplants, many short-term progenitors contributed to recipient PB regardless of donor age at four weeks post-transplant[23,38-40] (Figure 4B). RU numbers decreased over time as these progenitors exhausted their reconstituting potential for all PB lineages[23,38-40] (Figure 4B, Supplemental Figure 4A-B). Counterintuitively, PB RUs trended higher in recipients of aged BM *versus* recipients of young BM (Figure 4B, Supplemental Figure 4A). Consistently, reconstituted HSC of aged BM recipients displayed greater clonal

complexity than recipients of young BM (Figure 4C). Phenotypic HSC are known to accumulate in aged BM[26,27,41-44]. Indeed, a 10-fold increase in phenotypic HSC numbers was apparent in aged *Conf-VE*^{Cre} mice relative to young mice (Supplemental Figure 6A). Thus, the repopulating activity of phenotypic aged HSC appears about half that of young HSC (ratio of estimated RUs divided by the HSC number), consistent with previous reports (Supplemental Figure 6B)[45,46]. Thus, although the phenotypic HSC compartment expands with age, its activity is compromised relative to young HSC and many more aged clones are recruited to reconstitute homeostasis.

Serial transplantation dramatically reduces clonal diversity

Continued serial transplantation of aged and young BM reproducibly resulted in the dominance of a single *Confetti* color in reconstituted PB (Figure 5), suggesting oligoclonality. Accordingly, in secondary transplants of aged and young *Conf-VE*^{Cre}-BM, we observed a loss of clonal diversity in the CD45.2^{+} PB (including myeloid and lymphoid lineages) and HSPC (Figure 4B-C, Supplemental Figure 4B).

As the *Confetti* formula cannot accurately estimate the clonal complexity of an oligoclonal system[23], we developed an alternate strategy to quantify this progressive loss of complexity in subsequent transplants, focusing on the frequency of the most prevalent color as an indicator of clonal diversity expressed as percent of total (Figure 4D, Supplemental Figure 4C). There was no difference in the rate that young and old serially transplanted BM achieved clonal dominance in the HSC, MPP and myeloid compartments (Figure 4D, Supplemental Figure 4C). The differences observed in B- and

T-cell lineages are probably due to the earlier myeloid bias developed by the aged BM and that depletes the aged BM from the lymphoid lineages, precluding a proper comparison (Supplemental Figure 4C, Supplemental Figure 6C). Thus, serial transplantation steadily and dramatically reduces the clonal diversity of transplanted BM, regardless of the age of the primary donor.

Serial transplantation exacerbates clonal instability

To examine the flux of HSC output during serial transplantation, we again analyzed the behavior of "*Confetti*-pooled-clones" in individual mice (Figure 5). Dramatic expansions and constrictions of PB pooled-clones were apparent throughout serial transplantation of young BM (YFP and RFP in Groups A and B in Figure 5, Figure 6A-B, Supplemental Figures 5Ai-ii-3Di-ii). Further, in Group A, GFP-pooled-clones steadily increased in frequency in HSC during serial transplantation (Figure 5, Figure 6D and Supplemental Figure 5Biv). In contrast, the sudden expansion of GFP-pooled clones in the tertiary and quaternary PB of Group B recipients was never apparent in recipient HSC and MPP (Figure 5, Supplemental Figure 5B). For example, the secondary Group B recipient whose BM was transplanted into tertiary recipients had predominantly CFP^+ HSC. However, the frequency of these CFP-pooled-clones constricted dramatically in tertiary recipient PB by 16 weeks post-transplant and were a minority fraction in tertiary HSC, which was overtaken by YFP-pooled clones (Figure 5). In Groups D-F (Figure 5), which were serially transplanted with aged BM, large expansions of GFP-pooled-clones were mostly followed by constrictions (Figures 5, 6B, Supplemental Figure 5B). This supports the presence of small HSC clones with large contribution to PB. For example, the

distribution of PB pooled clones in Groups D-F secondary recipients were not reflected in their MPP and HSC (Figure 5, Supplemental Figure 5). In total, these data suggest PB and HSC clonal instability during serial transplantation.

Serially transplanted aged BM bears a heavier mutation load than serially transplanted young BM

Confetti-labeling suggests that serial transplantation of BM results in a loss of clonal complexity (Figure 4). By quaternary transplants, the majority of reconstituted blood is only one or two *Confetti* colors (Figure 5). To confirm clonal hematopoiesis, we performed WES on CD45.2^{+} BM labeled with individual *Confetti* colors (*i.e. Confetti*-clones) isolated by FACS from quaternary recipients of CD45.2^{+} *Conf-VE*^{Cre} aged or young BM. 11 *Confetti*-clones were sequenced: four isolated from recipients of young BM (Groups A-B) and seven from recipients of aged BM (Groups D-F) (Figure 5, 7, Table 1, Supplemental Tables 2-3). To ensure identification of true somatic mutations, at least two *Confetti* clones labeled with different colors were isolated from each transplant Group. Since *Confetti* clones in each Group originate from the same initial donor, somatic mutations acquired either during aging or serial transplantation can be distinguished from polymorphisms by comparing independent *Confetti* clones within a Group.

WES revealed 27 mutations (23 missense and 4 nonsense) that change the amino acid sequences (Table 1, Supplemental Tables 2-3). Five aged *Confetti* clones (O-1, O-3, O-4, O-7, O-11) acquired mutations with variant allele frequencies (VAF) close to 50%,

consistent with monoclonal hematopoiesis (Supplemental Table 3). For example, virtually all cells in O-4 carried a *Cdr1* mutation (VAF=53%), yet this variant was not observed in O-3 which received cells from the same primary donor. Interestingly, O-4 also harbored a sub-clone, as half of the sample carried a *Npy2r* mutation (VAF=25.9%) (Supplemental Table 3). Two aged *Confetti* clones (O-2, O-6) were oligoclonal (*e.g.* O-2 was composed of at least two clones (VAFs=10.4% and 14.9%)) (Supplemental Table 3). Two of four young *Confetti* clones (Y-2 and Y-3) were clonal (VAF=44% for each) or oligoclonal (Y-1, subclones were detected with VAFs=16.7% and 13.9%, Supplemental Table 3). Interestingly, the average counts of sample-specific mutations *per* transplant event (including missense, nonsense, silent and those outside the coding regions) in aged *Confetti* clones (4.2 mutations/transplant event) exceeded those of young *Confetti* clones (1.4 mutations/transplant event, p=0.02, Figure 7A). These data suggest that most mutations are acquired during aging or alternatively that aged HSC are more susceptible to mutagenesis under repeated stress.

To distinguish between these possibilities, we performed WES on *Confetti*-labeled young or aged BM isolated from primary recipients 16 months post-transplant or quaternary recipients four months post-transplant that were transplanted with cells from the same primary donor (Figure 7B). Comparing these primary and quaternary samples allowed us to assess the effect of time and time+repeated serial transplantation. If the observed mutations accumulated during the aging prior to transplant, then similar mutations should be observed in both cases. Clones of the same Confetti color within each transplant group (Two young clones (Y-5 and Y-6) and four aged clones (O-5, O-8, O-9 and O-10) were

sequenced (Supplemental Table 2). WES showed no overlap in mutations detected in primary versus quaternary samples (Supplemental Table 2). These data support a model in which most quaternary mutations are acquired during serial transplantation and aged BM is more susceptible to mutation during intense hematopoietic stress. Alternatively, small undetectable clones in primary samples may have been favored by serial transplantation.

We assessed if detected mutations were previously identified as variants in hematologic disease or cancer using Pecan PIE (Pathogenicity Information Exchange) (https://pecan.stjude.cloud/pie)[47]. A nonsense mutation in the B-cell CLL/lymphoma 11b (*Bcl11b*) locus (c. 610 C>T transition) has been implicated in T-ALL leukemogenesis. Low *BCL11b* expression correlates with poor prognosis in T-ALL patients[48,49,50]. We also identified a missense damaging mutation (Cys223Tyr) in a conserved, putative Ca^{+2} binding domain of the *Notch3* locus (Cys222 in the human protein) [51-53]. Elevated *NOTCH3* is seen in most T-ALL cases (Table 1 and Supplemental Table 3) [54]. A C>T transition resulted in p379Arg->Trp in protein tyrosine phosphatase receptor type (*Ptprr*). Eleven *PTPRR* R376 mutations have been reported in carcinomas and melanomas[47]. In addition, a C>T transition observed in the Neuropeptide Y receptor Y2 (*Npy2r*) has also been seen in carcinoma patients (Arg82Cys)[55, 47]. A G>A transversion in the Histone cluster 1, H2ac (*Hist1h2ac*) leading to an Arg33Trp was also observed. Reduced expression of *Hist1h2ac* correlates with increased cell proliferation[56,57]. Finally, we observed a frameshift deletion in Topoisomerase (DNA) II beta (*Top2b*), a target for several anticancer drugs[58,59].

In sum, WES of young and aged *Confetti* clones confirmed oligoclonal hematopoiesis and suggest that aged HSC may be hypersensitive to mutation when subjected to hematopoietic stress.

Discussion

We comprehensively examined the global clonal complexity of the murine hematopoietic system throughout life during steady state hematopoiesis. Although the presence of over-represented clones in aged PB is known, we showed for the first time that aging correlates with a global loss of clonal diversity in the entire blood system. These data caution against the use of aged donors for HSC transplantation. We also visualized the dynamics of clonal instability during native hematopoiesis and extended previous reports on aged HSC clones[15]. Our study further illuminated the effect of serial transplantation on hematopoietic clonal complexity driving a clonal collapse of reconstituted blood. Finally, we identified mutations that may confer a selective advantage during hematopoietic stress.

Here, we utilized a novel, non-invasive approach that depends on the observed MtMV in *Confetti* color distribution in cell populations. We previously validated the fidelity of this approach for estimating clonal numbers and reconstituting events in the blood system both during ontogeny and transplantation[23]. The behavior of individual clones are not tracked in this approach. Rather, much like classic limiting dilution transplantation assays based on Poisson statistics[34,60], MtMV is a statistical, indirect measure of clonal content and populations. Thus, an important caveat is that if a cell population consistently contains clones too small to perturb the distribution of *Confetti*-colors in individual mice, those clones are essentially 'hidden' from MtMV measurements. However, this caveat can be mitigated by increasing the size of mouse cohorts and numbers of cells analyzed. Further, with respect to aged HSC, these small 'hidden' clones can reflect important

biology, which is discussed at length below. MtMV is also influenced by cellular behavior (*i.e.* changes in the number of clones actively contributing to blood compartments). Many variables can influence the behavior of cells overtime (*e.g.* stress, infection, inflammation, epigenetic remodeling). Behavioral changes with age reflect the cumulative effect of these many variables on cells (and systems) throughout life. Here, we applied the MtMV in *Confetti* color distribution to measure the sum total effect of these insults on the blood and observed a loss of actively contributing clones in most blood compartments (Figure 1 and Supplemental Figure 1). Further experimentation will be necessary to decipher the biology driving changes in active clone numbers in aged blood.

Aging is accompanied by a large expansion in phenotypic HSC (Supplemental Figure 6A)[26,27,41-44] and a 20-fold decrease in transplantable HSC (Supplemental Figure 6B)[8,36-40,53,55-56 61]. The precipitous drop in HSC clonal complexity with age suggests that the expansion of phenotypic HSC results from just a few clones with a selective advantage, as suggested for CHIP[1,8]. Further, this loss of HSC complexity does not correlate in magnitude with the loss of clonal complexity seen in PB (Figure 4B-C, Supplemental Figure 1D). As aged HSC display poor repopulating activity relative to young HSC (Supplemental Figure 6B)[61], they are likely also compromised in their contribution to native hematopoiesis. Indeed, the BM frequency of expanded aged HSC *Confetti* pools is often not reflected in the blood, suggesting compromised output. We repeatedly observed aged PB GFP-pooled clones that were undetectable in BM (*e.g. Conf-E2a*^{Cre} #4; *Conf-Flk1*^{Cre} #6; *Conf-VE*^{Cre} #6, *Conf-Vav1*^{Cre} #6; Figure 3B), consistent with the model that

small 'young-like' HSC clones actively support aged PB, as proposed by de Haan and Lazare[8]. Although, in our study, we cannot measure the precise composition of clonal pools. None-the-less, very likely, only HSC clones that have not expanded dramatically preserve their functional potential and aged native hematopoiesis is maintained by a reduced pool of HSC clones[8,62]. Thus, although PB complexity drops with age, this drop is not equivalent to that seen in HSC. The pathological significance of harboring large numbers of phenotypic HSC compromised in differentiative potential is unclear. This may contribute to the selection of PB clones in elderly CHIP patients.

Our study complements a recent report estimating that about 50,000-200,000 HSC contribute to the blood at any given moment in middle-aged individuals[63]. 16-20 month old mice are equivalently middle-aged and did not display a loss of PB clonal complexity (Figure1C). It would be interesting to assess if the 30% drop in complexity seen in our study is conserved in an elderly (>80 years) individual. However, this may be difficult to detect, given the large range of contributing HSC reported in Lee-Six *et al*[63].

HSC are heterogeneous[36,42,64-67]. Aging is accompanied by delay in HSC cell *division ex vivo*, as previously described[68], and a loss of multipotency (Figure 3A), which suggests a global decline in HSC function. This decline could stem from increasing HSC functional heterogeneity or from a homogeneous loss of HSC function. Reduced correlation in *Confetti*-labeling patterns between BM HSPCs with age supports a model of increased heterogeneity (Figure 3C). To preserve *Confetti* color distribution between two BM compartments: 1) the immature compartment must evenly contribute to the downstream

compartment, 2) cell expansion and death must be evenly distributed across compartments and 3) these requirements must hold for any intermediates. Deviation from these requirements would weaken *Confetti* color correlations between compartments (*i.e.* functional heterogeneity in HSPCs negatively impacts the preservation of *Confetti* color distribution between populations). Thus, we favor a model in which aging increases HSC functional heterogeneity (Figure 3A, Figure 3C).

Interestingly, HSC and MPP were highly correlated in aged mice (Figure 3Cii-iii). It has been proposed that MPP support native hematopoiesis with rare contribution from HSC[19,20], which suggests that aged MPP emerge from HSC early in life or that HSC steadily (but rarely) contribute to MPP. This would also require MPP and HSC to preserve identical relative rates of symmetric and asymmetric cell division throughout life (*i.e.* to preserve *Confetti* color distributions after a long separation). A simpler model is that HSC actively and evenly generate MPP throughout life, consistent with the classic model of hematopoieisis[21]

We also examined the effect of age and stress on HSC function. Primary transplantation of aged BM required recruitment of larger clone numbers than young BM to re-establish hematopoietic homeostasis (Figure 4B-C, Supplemental Figure 6D), likely because aged HSC display less repopulating activity/cell than young HSC. Repeated serial transplantation drove a clonal collapse of the blood in both aged and young mice (Figure 4-6). Our data highlights significant differences between native and stress hematopoiesis (Figures 1, 4-5, Supplemental Figures 1D and 4). Stress (*i.e.* transplantation) dramatically

impacts the diversity of clones contributing to hematopoiesis (Figure 4-5, Supplemental Figures 4). Although clonal complexity also falls during native hematopoiesis (Figure 1, Supplemental Fig. 1D), this loss is more gradual and smaller in magnitude than that seen post-transplant. Thus, to fully appreciate hematopoietic clonal dynamics, it is critical to interrogate both native and stress hematopoiesis.

We identified mutations in six genes (*i.e. Bcl11b, Hist1h2ac, Npy2r, Notch3, Ptprr* and *Top2b*) that may confer a selective advantage to HSCs during aging and/or serial transplantation (Table 1 and Supplemental Table 3). *Bcl11b* regulates thymocyte development[48,49]. Structural variants and mutations in *BCL11B* have been seen in AML, pediatric and adult T-ALL and T/myeloid acute bi-lineage leukemia[51,69-77,78,79]. PTPRR is a protein tyrosine phosphatase linked to colorectal and cervical cancer[80,81,82]. NOTCH3 mutations have been causally linked to cerebral autosomal dominant arteriopathy[83]. High levels of *NOTCH3* are detected regularly in T-ALL[54, 84]. Variations in the levels of HIST1H2AC might contribute to carcinogenesis[56,57]. TOP2B is a DNA topoisomerase that alleviates topological stress during DNA replication and transcription[85]. *TOP2B* mutations correlate with drug resistance and chromosome translocations in therapy-induced leukemia[58,59,86-89]. Finally, *Npy2r* (a G-protein coupled receptor) regulates memory[90,91]. We did not detect the most frequent mutations in CHIP patients (*e.g. Dnmt3a, Asxl1, Tet2; total frequency≈30%)*. This could simply be due to the small number of clones interrogated in our study[6,7].

In summary, our non-invasive approach constitutes, to our knowledge, the first study of the dynamics of the absolute clonal complexity of steady state hematopoiesis during a natural mammalian lifespan. Here, aging resulted in a global loss of clonal complexity and intense repeated hematopoietic stress compromised HSC self-renewal, regardless of age, ending in clonal collapse and loss of lymphoid potential. Moreover, we identified novel mutations that potentially select for HSC capable of extensive self-renewal in the face of hematopoietic stress. Understanding the functional significance of these mutations could shed light on similar processes in human clonal hematopoiesis and warrants further investigation.

Acknowledgements

We thank W. Clements, J. Klco, E. Obeng, A. Morales and the rest of the McKinney-Freeman laboratory and Department of Hematology at St. Jude Children's Research Hospital for critical discussions and reading of the manuscript; D. Ashmun, S. Schwemberger, and J. Laxton for FACS support; C. Davis-Goodrum, Krista Millican, Amber Reap and C. Savage for help with injections and timed pregnancies. *Vav1*-Cre$^{+/T}$ mice were a gift from the laboratory of Thomas Graf (Center for Genomic Regulation, Spain) by way of Dr. Nancy Speck (University of Pennsylvania, PA USA). *VE-Cadherin*-Cre$^{+/T}$ mice were a gift from the laboratory of Dr. Guillermo Oliver (Northwestern University, IL USA).

This work was supported by the American Society of Hematology (S.M.-F.), the Hartwell Foundation (S.M.-F.), the NIDDK (R01DK104028, S.M.-F.) and the American Lebanese Syrian Associated Charities (S.M.-F.). The authors have no conflicting financial interests.

Author Contributions

M.G. designed the study, performed and analyzed transplants, collected and analyzed data, and wrote the paper. T.H. contributed to study design, collected data and wrote the paper. D.F. performed statistical analysis for estimating cell numbers and tracking clonal complexity evolution, analyzed data, contributed to study design, and wrote relevant sections of paper. A.C. analyzed *Confetti*+ blood and resulting data. Y-D.W. and G.W. performed whole exome sequencing analysis. G.K. and W.B. performed statistical analyses, S.M.-F. designed the study, analyzed data, and wrote the paper. All authors discussed the results and commented on the manuscript.

Correspondence and request for materials should be addressed to S.M.-F. (Shannon.mckinney-freeman@stjude.org).

Conflict of Interest Disclosure

The authors have no conflicting financial interests.

Table 1. Mutations identified that altered amino acid sequences

Symbol	Reference	Allele	Coding / amino acid change	Group	Mutation Type	Conserved region in human[1] genome	Predicted functional effect[2]
Csmd1	C	T	NM_053171:c.5755G>A,p.Ala1919Thr	Young	missense	No	N/A
Lmln	C	T	NM_172823:c.1597C>T,p.Gln533*	Young	nonsense	Yes	Damaging
Mrgpra6	G	A	NM_001308537:c.799C>T,p.Arg267Trp	Young	missense	No	N/A
Sidt2	G	C	NM_172257:c.[1062C>G],p.[Tyr354*]	Young	nonsense	Yes	Stop gain
Slc5a9	C	T	NM_145551:c.298G>A,p.Gly100Ser	Young	missense	Yes	Damaging
Ahnak	C	T	NM_009643:c.[3092C>T],p.Pro1031Leu	Old	missense	Yes	Damaging
Bcl11b	G	A	NM_021399:c.610C>T,p.Gln204*	Old	nonsense	Yes	Damaging
Carm1	A	G	NM_021531:c.[1441A>G],p.[Thr481Ala]	Old	missense	Yes	Benign
Cdr1	G	A	NM_001166658:c.892C>T,p.Arg298Trp	Old	missense	No	N/A
Hist1h2ac	G	A	NM_178189:c.97C>T,p.Arg33Trp	Old	missense	Yes	Damaging
Grin3a	A	-	NM_001033351:c.[1797delT],p.[Ile599fs]	Old	deletion	Yes	Frameshift
Itpkb	A	G	NM_001081175:c.2521A>G,p.Lys841Glu	Old	missense	Yes	Benign
Notch3	C	T	NM_008716:c.668G>A,p.Cys223Tyr	Old	missense	Yes	Damaging
Npy2r	G	A	NM_008731:c.244C>T,p.Arg82Cys	Old	missense	Yes	Damaging
Olfr1111	G	T	NM_146593:c.20C>A,p.Thr7Asn	Old	missense	Yes	Probably Damaging
Pde6a	G	A	NM_146086:c.161G>A,p.Ser54Asn	Old	missense	Yes	Benign
Prb1	G	T	NM_053251:c.702C>A,p.Asp234Glu	Old	missense	No	N/A
Ptprr	C	T	NM_011217:c.1135C>T,p.Arg379Trp	Old	missense	Yes	Damaging
Rapgef1	G	A	NM_001039086:c.2164G>A,p.Glu722Lys	Old	missense	No	N/A
Rnf6	C	T	NM_028774:c.1003G>A,p.Val335Ile	Old	missense	No	N/A
Scn2a	A	C	NM_001099298:c.5480A>C,p.Asp1827Ala	Old	missense	Yes	Benign
Tada1	T	G	NM_030245:c.803T>G,p.Leu268Arg	Old	missense	Yes	Benign
Tjp1	A	G	NM_009386:c.4991T>C,p.Ile1664Thr	Old	missense	Yes	Benign
Top2b	G	-	NM_009409:c.1487delG,p.Gly497fs	Old	deletion	Yes	Frameshift
Vmn2r49	G	A	NM_001105156:c.647C>T,p.Pro216Leu	Old	missense	No	N/A
Zcwpw1	G	A	NM_001005426:c.34G>A,p.Glu12Lys	Old	missense	No	N/A
Zfp735	G	T	NM_001126489:c.510G>T,p.Lys170Asn	Old	missense	No	N/A

Gene ID, nucleotide change, amino acid change, age group, type of mutation, conservation in human sequence and predicted functional consequences in the protein function are indicated. Mutated genes with predicted damaging consequences are highlighted in red. [1] Homologous region was identified in Human protein. [2] Predicted based on Polyphen-2 tool.

Figure Legends

Figure 1. The global clonal complexity of the hematopoietic system declines with age.

a, Schematic of experimental approach. The clonal complexity of the PB and BM of cohorts of *Conf-E2a*^{Cre}; *Conf-VE*^{Cre}; *Conf-Flk1*^{Cre} and *Conf-Vav1*^{Cre} mice were examined at two, seven, 12, 16, 20, 24 and 26 months of age. See Supplemental Figure 1a-b for schematic of *Confetti* allele and *Confetti* color flow cytometry gating strategy. **b**, **i and ii,** Schematic of the inverse relationship between numbers of initially labeled events and Mouse-to-Mouse Variance (MtMV) in the distribution of *Confetti* colors. **c, i,** Analysis of the clonal complexity of the PB in cohorts of mice from two to 26 months of age. At two months old: *Conf-E2a*^{Cre} (n=14), *Conf-VE*^{Cre}(n=13), *Conf-Flk1*^{Cre}(n=7), *Conf-Vav1*^{Cre} (n=11). At 26 months old, *Conf-E2a*^{Cre} (n=10), *Conf-VE*^{Cre}(n=5), *Conf-Flk1*^{Cre}(n=6), *Conf-Vav1*^{Cre} (n=9). **ii,** Average PB clonal complexity of *Conf-Flk1*^{Cre}, *Conf-VE*^{Cre} and *Conf-Vav1*^{Cre} mice overtime relative to two months of age. Error bars indicated standard deviation. **d, i,** The clonal complexity of the major BM HSPC from cohorts of mice were calculated at two and 26 months of age from previously cKit^{+} enriched BM. At two months, *Conf-E2a*^{Cre} (n=3), *Conf-VE*^{Cre}(n= 6), *Conf-Flk1*^{Cre}(n=7), *Conf-Vav1*^{Cre} (n= 8). At 26 months, *Conf-E2a*^{Cre} (n=7), *Conf-VE*^{Cre}(n=4), *Conf-Flk1*^{Cre} (n= 5), *Conf-Vav1*^{Cre} (n=5). **ii,** Average BM HSPC clonal complexities of *Conf-Flk1*^{Cre}, *Conf-VE*^{Cre} and *Conf-Vav1*^{Cre} mice overtime relative to two months of age. Error bars indicate standard deviation. (* p-value<0.05; # p-value<0.1). Source data are provided in Supplemental Table 1. **iii,** Schematic of the consequences of aging on HSC and PB clonal complexity. The absolute number of phenotypic HSC increase with age (Supplemental Fig. 6A) due

585 to the expansion of functionally impaired clones. In aged mice, "young-like" minimally-
586 expanded HSC contribute disproportionately to PB, resulting in a less dramatic decrease
587 in PB clonal complexity.
588
589 **Figure 2. Analysis of pooled clones over time reveals instability in the clonal**
590 **composition of PB during native hematopoiesis.**
591 **a,** Visualization of the distribution of GFP, YFP, RFP and CFP in the PB of
592 representative *Conf-E2a*^{Cre}, *Conf-VE*^{Cre}, *Conf-Flk1*^{Cre}, *Conf-Vav1*^{Cre} mice at two, seven,
593 12, 16, 20, 24 and 26 months of age. **b,** Fold change in the %GFP relative to the
594 preceding time-point. Each line represents an independent mouse. Mice from all four
595 cohorts are shown. *Conf-E2a*^{Cre} (n=9), *Conf-VE*^{Cre} (n=7), *Conf-Flk1*^{Cre} (n=6), *Conf-*
596 *Vav1*^{Cre} (n=10). Evolution of %GFP for individual PB lineages is shown in Supplemental
597 Figure 2 for each mouse, each mouse strain and without normalization. Source data are
598 provided in Supplemental Table 1.
599
600 **Figure 3. Aging functionally compromises HSC and erodes the lineage relationships**
601 **between bone marrow compartments during native hematopoiesis.**
602 **a,** Single HSC from three independent young or aged mice were individually plated in
603 96-well plates in media that supports HSC expansion (**i,** n=44-67 clones analyzed/mouse**)**
604 or differentiation media (**ii,** n=27-41 clones were analyzed/mouse). **i,** Division kinetics
605 for each well were tracked, % of cumulative number of divisions are shown. **ii,** % of
606 clones that generate one, two, three or four myeloid lineages (See Supplemental Figure
607 3A). Averages are shown, error bars represent standard deviation (# p-value < 0.1). **b,**

Distribution of *Confetti* colors in PB and BM in young (age two months) and old (age 26 months) mice. Three representative examples are shown for each mouse strain at each time-point. **c,** Heatmaps summarize the correlation of *Confetti* color distribution between different hematopoietic compartments in young (**i,** age two months) and old (**ii,** age 26 months) mice. Heatmaps depict the Pearson's correlation coefficient between two cell compartments. At two months old: *Conf-E2a*^{Cre} (n=14), *Conf-VE*^{Cre}(n=13), *Conf-Flk1*^{Cre} (n=7), *Conf-Vav1*^{Cre} (n=11). At 26 months old, *Conf-E2a*^{Cre} (n=10), *Conf-VE*^{Cre}(n=5), *Conf-Flk1*^{Cre}(n=6), *Conf-Vav1*^{Cre} (n=9). **iii,** Correlation values of BM compartments relative to HSC at 2 and 26 months of age. Paired t test of correlation coefficient of cells *vs*. HSC indicate that the correlations are significantly reduced with age (p-value = 0.03). See also Supplemental Figure 3B. Source data are provided in Supplemental Table 1.

Figure 4. Serial transplantation of aged and young bone marrow results in a loss of clonal complexity

a-d, CD45.2^{+} *Conf-VE*^{Cre} BM was serially transplanted. **a,** Schematic of serial transplantation of CD45.2^{+} *Conf-VE*^{Cre} BM. For primary transplant, 5x10^{6} BM cells were transplanted from young (age two months) or old (age 24 months) donors into distinct cohorts of primary CD45.2^{+}/CD45.1^{+} recipients. For serial transplants, 5x10^{6} BM cells were transplanted. For each age group (young and old) at least three independent donor mice were transplanted into distinct recipient cohorts. Each cohort was composed of at least five mice and was transplanted with an independent donor. **b,** Recipient PB was analyzed for the distribution of *Confetti* colors in their PB at four, 10 and 16 weeks post-transplant. MtMV was used to estimate the number of repopulating units (see Methods).

631 Primary and secondary transplants are shown. (See Supplemental Figure 4 for additional
632 cell doses transplanted in primary transplants and PB lineages. See also Figure 5). **c,**
633 Recipient BM HSC were examined at four months post-transplant for the MtMV in the
634 *Confetti* colors. (See Supplemental Figure 6D for additional BM HSPC compartments).
635 **b-c,** Averages are shown, error bars denote standard deviation (*p-value<0.05; #p-
636 value<0.1) **d,** The median frequency of the most prevalent color is shown for the PB
637 (four and 16 weeks) and MPP and HSC (16 weeks) for each transplantation stage.
638 Whisker plots show interquartile range. ANOVA analysis was run to test for the
639 statistical significance of the transplantation stage and age for each cell type. Age did not
640 result in statistical differences for any cell type. Transplantation stage had a significant
641 effect in all cell types (p-values<0.05) except HSC. (* p-value<0.05). **b-d,** each bar or
642 point represents the average or median obtained from at least three independent cohorts
643 of mice (each cohort n≥5) from three independent initial young or old donors. Source
644 data are provided in Supplemental Table 1.
645
646 **Figure 5. Serial transplantation of aged and young bone marrow drives clonal**
647 **collapse of reconstituted hematopoiesis**
648 **a-b,** Pie graphs show the distribution of *Confetti* colors in the nucleated cells of the PB,
649 MPP and HSC of each recipient. Each pie graph represents an independent mouse. Each
650 column of pie charts refers to the same mouse. Vertical arrows indicate donor mice for
651 the subsequent transplant. Results are shown at four and 16 weeks post-transplant. **a,**
652 Serial transplantation from young primary BM donors. **b,** Serial transplantation from old
653 primary BM donors. Data related to Figure 4a-c. Source data are provided in

Supplemental Table 1. Data for HSC and MPP at the quaternary stage is not shown as they were used for WES.

Figure 6. Labeled pooled-clones revealed clonal instability during serial transplantation

The average frequency of CFP-, YFP-, RFP- or GFP-labeled pooled-clones in the PB at four **(a)** and 16 weeks **(b)** and in MPP at 16 weeks **(c)** and HSC **(d)** at 16 weeks throughout transplantation. Results are shown for each transplanted group (#A-F). Related to Figure 5. Whisker plots show the interquartile range. n≥5 for each transplanted mouse cohort. See Supplemental Figure 5 for the distribution of all pooled-clones. Source data are provided in Supplemental Table 1.

Figure 7. Aged *Confetti* clones exhibit higher mutational rates than young *Confetti* clones

Transplanted *Conf-VE*^{Cre} BM from aged or young donors was either maintained for 16 months in primary recipients or serially transplanted every four months for a total of 16 months. *Confetti* sorted clones were subjected to whole-exome-sequencing. **a,** Experimental schematic. **b,** Whole exome sequencing of aged (n=7) and young (n=4) sorted *Confetti* clones after serial transplantation. Mutation analysis revealed that aged clones accumulated a significantly higher number of mutations than young clones when serially transplanted (* p-value < 0.05) **c,** Whole exome sequencing of aged (n=4) and young (n=2) sorted *Confetti* clones 16 months post-primary transplant. No overlap was observed in mutations detected after primary transplant compared to repeated

transplantation (Please see Supplemental Tables 2-3). **(b)**. See also Table 1 and Methods for experimental details.

References

1 Goodell, M. A. & Rando, T. A. Stem cells and healthy aging. *Science* **350**, 1199-1204, doi:10.1126/science.aab3388 (2015).

2 Lopez-Otin, C., Blasco, M. A., Partridge, L., Serrano, M. & Kroemer, G. The hallmarks of aging. *Cell* **153**, 1194-1217, doi:10.1016/j.cell.2013.05.039 (2013).

3 Shaw, A. C., Joshi, S., Greenwood, H., Panda, A. & Lord, J. M. Aging of the innate immune system. *Curr Opin Immunol* **22**, 507-513, doi:10.1016/j.coi.2010.05.003 (2010).

4 Zink, F. *et al.* Clonal hematopoiesis, with and without candidate driver mutations, is common in the elderly. *Blood* **130**, 742-752, doi:10.1182/blood-2017-02-769869 (2017).

5 Xie, M. *et al.* Age-related mutations associated with clonal hematopoietic expansion and malignancies. *Nat Med* **20**, 1472-1478, doi:10.1038/nm.3733 (2014).

6 Jaiswal, S. *et al.* Age-related clonal hematopoiesis associated with adverse outcomes. *N Engl J Med* **371**, 2488-2498, doi:10.1056/NEJMoa1408617 (2014).

7 Genovese, G. *et al.* Clonal hematopoiesis and blood-cancer risk inferred from blood DNA sequence. *N Engl J Med* **371**, 2477-2487, doi:10.1056/NEJMoa1409405 (2014).

8 de Haan, G. & Lazare, S. S. Aging of hematopoietic stem cells. *Blood* **131**, 479-487, doi:10.1182/blood-2017-06-746412 (2018).

9 van den Akker, E. B. *et al.* Uncompromised 10-year survival of oldest old carrying somatic mutations in DNMT3A and TET2. *Blood* **127**, 1512-1515, doi:10.1182/blood-2015-12-685925 (2016).

10 Acuna-Hidalgo, R. *et al.* Ultra-sensitive Sequencing Identifies High Prevalence of Clonal Hematopoiesis-Associated Mutations throughout Adult Life. *Am J Hum Genet* **101**, 50-64, doi:10.1016/j.ajhg.2017.05.013 (2017).

11 Jaiswal, S. *et al.* Clonal Hematopoiesis and Risk of Atherosclerotic Cardiovascular Disease. *N Engl J Med* **377**, 111-121, doi:10.1056/NEJMoa1701719 (2017).

12 Champion, K. M., Gilbert, J. G., Asimakopoulos, F. A., Hinshelwood, S. & Green, A. R. Clonal haemopoiesis in normal elderly women: implications for the myeloproliferative disorders and myelodysplastic syndromes. *Br J Haematol* **97**, 920-926 (1997).

13 Busque, L. *et al.* Nonrandom X-inactivation patterns in normal females: lyonization ratios vary with age. *Blood* **88**, 59-65 (1996).

14 Fuster, J. J. *et al.* Clonal hematopoiesis associated with TET2 deficiency accelerates atherosclerosis development in mice. *Science* **355**, 842-847, doi:10.1126/science.aag1381 (2017).

15 Verovskaya, E. *et al.* Heterogeneity of young and aged murine hematopoietic stem cells revealed by quantitative clonal analysis using cellular barcoding. *Blood* **122**, 523-532, doi:10.1182/blood-2013-01-481135 (2013).
16 Ashcroft, P., Manz, M. G. & Bonhoeffer, S. Clonal dominance and transplantation dynamics in hematopoietic stem cell compartments. *PLoS Comput Biol* **13**, e1005803, doi:10.1371/journal.pcbi.1005803 (2017).
17 Sieburg, H. B., Rezner, B. D. & Muller-Sieburg, C. E. Predicting clonal self-renewal and extinction of hematopoietic stem cells. *Proc Natl Acad Sci U S A* **108**, 4370-4375, doi:10.1073/pnas.1011414108 (2011).
18 Ganuza, M. & McKinney-Freeman, S. Hematopoietic stem cells under pressure. *Curr Opin Hematol* **24**, 314-321, doi:10.1097/MOH.0000000000000347 (2017).
19 Sun, J. *et al.* Clonal dynamics of native haematopoiesis. *Nature* **514**, 322-327, doi:10.1038/nature13824 (2014).
20 Busch, K. *et al.* Fundamental properties of unperturbed haematopoiesis from stem cells in vivo. *Nature* **518**, 542-546, doi:10.1038/nature14242 (2015).
21 Sawai, C. M. *et al.* Hematopoietic Stem Cells Are the Major Source of Multilineage Hematopoiesis in Adult Animals. *Immunity* **45**, 597-609, doi:10.1016/j.immuni.2016.08.007 (2016).
22 Snippert, H. J. *et al.* Intestinal crypt homeostasis results from neutral competition between symmetrically dividing Lgr5 stem cells. *Cell* **143**, 134-144, doi:10.1016/j.cell.2010.09.016 (2010).
23 Ganuza, M. *et al.* Lifelong haematopoiesis is established by hundreds of precursors throughout mammalian ontogeny. *Nat Cell Biol* **19**, 1153-1163, doi:10.1038/ncb3607 (2017).
24 Hinge, A. *et al.* p190-B RhoGAP and intracellular cytokine signals balance hematopoietic stem and progenitor cell self-renewal and differentiation. *Nat Commun* **8**, 14382, doi:10.1038/ncomms14382 (2017).
25 Oguro, H., Ding, L. & Morrison, S. J. SLAM family markers resolve functionally distinct subpopulations of hematopoietic stem cells and multipotent progenitors. *Cell Stem Cell* **13**, 102-116, doi:10.1016/j.stem.2013.05.014 (2013).
26 Cho, R. H., Sieburg, H. B. & Muller-Sieburg, C. E. A new mechanism for the aging of hematopoietic stem cells: aging changes the clonal composition of the stem cell compartment but not individual stem cells. *Blood* **111**, 5553-5561, doi:10.1182/blood-2007-11-123547 (2008).
27 Sudo, K., Ema, H., Morita, Y. & Nakauchi, H. Age-associated characteristics of murine hematopoietic stem cells. *J Exp Med* **192**, 1273-1280 (2000).
28 Szilvassy, S. J., Humphries, R. K., Lansdorp, P. M., Eaves, A. C. & Eaves, C. J. Quantitative assay for totipotent reconstituting hematopoietic stem cells by a competitive repopulation strategy. *Proc Natl Acad Sci U S A* **87**, 8736-8740 (1990).
29 Kiel, M. J. *et al.* SLAM family receptors distinguish hematopoietic stem and progenitor cells and reveal endothelial niches for stem cells. *Cell* **121**, 1109-1121, doi:10.1016/j.cell.2005.05.026 (2005).

30 Sieburg, H. B. *et al.* The hematopoietic stem compartment consists of a limited number of discrete stem cell subsets. *Blood* **107**, 2311-2316, doi:10.1182/blood-2005-07-2970 (2006).
31 Kay, H. E. How Many Cell-Generations? *Lancet* **2**, 418-419 (1965).
32 Wilson, A. *et al.* Hematopoietic stem cells reversibly switch from dormancy to self-renewal during homeostasis and repair. *Cell* **135**, 1118-1129, doi:10.1016/j.cell.2008.10.048 (2008).
33 Foudi, A. *et al.* Analysis of histone 2B-GFP retention reveals slowly cycling hematopoietic stem cells. *Nat Biotechnol* **27**, 84-90, doi:10.1038/nbt.1517 (2009).
34 Harrison, D. E., Astle, C. M. & Lerner, C. Number and continuous proliferative pattern of transplanted primitive immunohematopoietic stem cells. *Proc Natl Acad Sci U S A* **85**, 822-826 (1988).
35 Takizawa, H., Regoes, R. R., Boddupalli, C. S., Bonhoeffer, S. & Manz, M. G. Dynamic variation in cycling of hematopoietic stem cells in steady state and inflammation. *J Exp Med* **208**, 273-284, doi:10.1084/jem.20101643 (2011).
36 Yu, V. W. C. *et al.* Epigenetic Memory Underlies Cell-Autonomous Heterogeneous Behavior of Hematopoietic Stem Cells. *Cell* **167**, 1310-1322 e1317, doi:10.1016/j.cell.2016.10.045 (2016).
37 Rios, A. C., Fu, N. Y., Lindeman, G. J. & Visvader, J. E. In situ identification of bipotent stem cells in the mammary gland. *Nature* **506**, 322-327, doi:10.1038/nature12948 (2014).
38 Jordan, C. T. & Lemischka, I. R. Clonal and systemic analysis of long-term hematopoiesis in the mouse. *Genes Dev* **4**, 220-232 (1990).
39 Purton, L. E. & Scadden, D. T. Limiting factors in murine hematopoietic stem cell assays. *Cell Stem Cell* **1**, 263-270, doi:10.1016/j.stem.2007.08.016 (2007).
40 Yang, L. *et al.* Identification of Lin(-)Sca1(+)kit(+)CD34(+)Flt3- short-term hematopoietic stem cells capable of rapidly reconstituting and rescuing myeloablated transplant recipients. *Blood* **105**, 2717-2723, doi:10.1182/blood-2004-06-2159 (2005).
41 Benz, C. *et al.* Hematopoietic stem cell subtypes expand differentially during development and display distinct lymphopoietic programs. *Cell Stem Cell* **10**, 273-283, doi:10.1016/j.stem.2012.02.007 (2012).
42 Dykstra, B., Olthof, S., Schreuder, J., Ritsema, M. & de Haan, G. Clonal analysis reveals multiple functional defects of aged murine hematopoietic stem cells. *J Exp Med* **208**, 2691-2703, doi:10.1084/jem.20111490 (2011).
43 Beerman, I. *et al.* Functionally distinct hematopoietic stem cells modulate hematopoietic lineage potential during aging by a mechanism of clonal expansion. *Proc Natl Acad Sci U S A* **107**, 5465-5470, doi:10.1073/pnas.1000834107 (2010).
44 Yamamoto, R. *et al.* Large-Scale Clonal Analysis Resolves Aging of the Mouse Hematopoietic Stem Cell Compartment. *Cell Stem Cell* **22**, 600-607 e604, doi:10.1016/j.stem.2018.03.013 (2018).
45 Morrison, S. J., Wandycz, A. M., Akashi, K., Globerson, A. & Weissman, I. L. The aging of hematopoietic stem cells. *Nat Med* **2**, 1011-1016 (1996).

46 Rossi, D. J. *et al.* Cell intrinsic alterations underlie hematopoietic stem cell aging. *Proc Natl Acad Sci U S A* **102**, 9194-9199, doi:10.1073/pnas.0503280102 (2005).
47 Zhang, J. *et al.* Germline Mutations in Predisposition Genes in Pediatric Cancer. *N Engl J Med* **373**, 2336-2346, doi:10.1056/NEJMoa1508054 (2015).
48 Liu, P., Li, P. & Burke, S. Critical roles of Bcl11b in T-cell development and maintenance of T-cell identity. *Immunol Rev* **238**, 138-149, doi:10.1111/j.1600-065X.2010.00953.x (2010).
49 Kominami, R. Role of the transcription factor Bcl11b in development and lymphomagenesis. *Proc Jpn Acad Ser B Phys Biol Sci* **88**, 72-87 (2012).
50 Bartram, I. *et al.* Low expression of T-cell transcription factor BCL11b predicts inferior survival in adult standard risk T-cell acute lymphoblastic leukemia patients. *J Hematol Oncol* **7**, 51, doi:10.1186/s13045-014-0051-y (2014).
51 Ramensky, V., Bork, P. & Sunyaev, S. Human non-synonymous SNPs: server and survey. *Nucleic Acids Res* **30**, 3894-3900 (2002).
52 Sunyaev, S., Ramensky, V. & Bork, P. Towards a structural basis of human non-synonymous single nucleotide polymorphisms. *Trends Genet* **16**, 198-200 (2000).
53 Sunyaev, S. *et al.* Prediction of deleterious human alleles. *Hum Mol Genet* **10**, 591-597 (2001).
54 Bellavia, D. *et al.* Combined expression of pTalpha and Notch3 in T cell leukemia identifies the requirement of preTCR for leukemogenesis. *Proc Natl Acad Sci U S A* **99**, 3788-3793, doi:10.1073/pnas.062050599 (2002).
55 Ammar, D. A. *et al.* Characterization of the human type 2 neuropeptide Y receptor gene (NPY2R) and localization to the chromosome 4q region containing the type 1 neuropeptide Y receptor gene. *Genomics* **38**, 392-398 (1996).
56 Singh, R. *et al.* Proteomic profiling identifies specific histone species associated with leukemic and cancer cells. *Clin Proteomics* **12**, 22, doi:10.1186/s12014-015-9095-4 (2015).
57 Singh, R. *et al.* Increasing the complexity of chromatin: functionally distinct roles for replication-dependent histone H2A isoforms in cell proliferation and carcinogenesis. *Nucleic Acids Res* **41**, 9284-9295, doi:10.1093/nar/gkt736 (2013).
58 Gieseler, F. *et al.* Topoisomerase II activities in AML and their correlation with cellular sensitivity to anthracyclines and epipodophyllotoxines. *Leukemia* **10**, 1177-1180 (1996).
59 Gieseler, F. *et al.* Topoisomerase II activities in AML blasts and their correlation with cellular sensitivity to anthracyclines and epipodophyllotoxines. *Leukemia* **10 Suppl 3**, S46-S49 (1996).
60 Harrison, D. E., Astle, C. M. & Stone, M. Numbers and functions of transplantable primitive immunohematopoietic stem cells. Effects of age. *J Immunol* **142**, 3833-3840 (1989).
61 Yilmaz, O. H., Kiel, M. J. & Morrison, S. J. SLAM family markers are conserved among hematopoietic stem cells from old and reconstituted mice and

markedly increase their purity. *Blood* **107**, 924-930, doi:10.1182/blood-2005-05-2140 (2006).
62 Bernitz, J. M., Kim, H. S., MacArthur, B., Sieburg, H. & Moore, K. Hematopoietic Stem Cells Count and Remember Self-Renewal Divisions. *Cell* **167**, 1296-1309 e1210, doi:10.1016/j.cell.2016.10.022 (2016).
63 Lee-Six, H. *et al.* Population dynamics of normal human blood inferred from somatic mutations. *Nature* **561**, 473-478, doi:10.1038/s41586-018-0497-0 (2018).
64 Morita, Y., Ema, H. & Nakauchi, H. Heterogeneity and hierarchy within the most primitive hematopoietic stem cell compartment. *J Exp Med* **207**, 1173-1182, doi:10.1084/jem.20091318 (2010).
65 Picelli, S. *et al.* Smart-seq2 for sensitive full-length transcriptome profiling in single cells. *Nat Methods* **10**, 1096-1098, doi:10.1038/nmeth.2639 (2013).
66 Muller-Sieburg, C. E., Cho, R. H., Karlsson, L., Huang, J. F. & Sieburg, H. B. Myeloid-biased hematopoietic stem cells have extensive self-renewal capacity but generate diminished lymphoid progeny with impaired IL-7 responsiveness. *Blood* **103**, 4111-4118, doi:10.1182/blood-2003-10-3448 (2004).
67 Dykstra, B. *et al.* Long-term propagation of distinct hematopoietic differentiation programs in vivo. *Cell Stem Cell* **1**, 218-229, doi:10.1016/j.stem.2007.05.015 (2007).
68 Flach, J. *et al.* Replication stress is a potent driver of functional decline in ageing haematopoietic stem cells. *Nature* **512**, 198-202, doi:10.1038/nature13619 (2014).
69 MacLeod, R. A., Nagel, S., Kaufmann, M., Janssen, J. W. & Drexler, H. G. Activation of HOX11L2 by juxtaposition with 3'-BCL11B in an acute lymphoblastic leukemia cell line (HPB-ALL) with t(5;14)(q35;q32.2). *Genes Chromosomes Cancer* **37**, 84-91, doi:10.1002/gcc.10194 (2003).
70 Przybylski, G. K. *et al.* Disruption of the BCL11B gene through inv(14)(q11.2q32.31) results in the expression of BCL11B-TRDC fusion transcripts and is associated with the absence of wild-type BCL11B transcripts in T-ALL. *Leukemia* **19**, 201-208, doi:10.1038/sj.leu.2403619 (2005).
71 De Keersmaecker, K. *et al.* Exome sequencing identifies mutation in CNOT3 and ribosomal genes RPL5 and RPL10 in T-cell acute lymphoblastic leukemia. *Nat Genet* **45**, 186-190, doi:10.1038/ng.2508 (2013).
72 De Keersmaecker, K. *et al.* The TLX1 oncogene drives aneuploidy in T cell transformation. *Nat Med* **16**, 1321-1327, doi:10.1038/nm.2246 (2010).
73 Satterwhite, E. *et al.* The BCL11 gene family: involvement of BCL11A in lymphoid malignancies. *Blood* **98**, 3413-3420 (2001).
74 Bezrookove, V. *et al.* A novel t(6;14)(q25-q27;q32) in acute myelocytic leukemia involves the BCL11B gene. *Cancer Genet Cytogenet* **149**, 72-76 (2004).
75 Oliveira, J. L. *et al.* Successful treatment of a child with T/myeloid acute bilineal leukemia associated with TLX3/BCL11B fusion and 9q deletion. *Pediatr Blood Cancer* **56**, 467-469, doi:10.1002/pbc.22850 (2011).

76 Abbas, S. *et al.* Integrated genome-wide genotyping and gene expression profiling reveals BCL11B as a putative oncogene in acute myeloid leukemia with 14q32 aberrations. *Haematologica* **99**, 848-857, doi:10.3324/haematol.2013.095604 (2014).
77 Gutierrez, A. *et al.* The BCL11B tumor suppressor is mutated across the major molecular subtypes of T-cell acute lymphoblastic leukemia. *Blood* **118**, 4169-4173, doi:10.1182/blood-2010-11-318873 (2011).
78 Wakabayashi, Y. *et al.* Bcl11b is required for differentiation and survival of alphabeta T lymphocytes. *Nat Immunol* **4**, 533-539, doi:10.1038/ni927 (2003).
79 Kamimura, K. *et al.* Haploinsufficiency of Bcl11b for suppression of lymphomagenesis and thymocyte development. *Biochem Biophys Res Commun* **355**, 538-542, doi:10.1016/j.bbrc.2007.02.003 (2007).
80 Alonso, A. *et al.* Protein tyrosine phosphatases in the human genome. *Cell* **117**, 699-711, doi:10.1016/j.cell.2004.05.018 (2004).
81 Menigatti, M. *et al.* The protein tyrosine phosphatase receptor type R gene is an early and frequent target of silencing in human colorectal tumorigenesis. *Mol Cancer* **8**, 124, doi:10.1186/1476-4598-8-124 (2009).
82 Su, P. H. *et al.* Epigenetic silencing of PTPRR activates MAPK signaling, promotes metastasis and serves as a biomarker of invasive cervical cancer. *Oncogene* **32**, 15-26, doi:10.1038/onc.2012.29 (2013).
83 Li, S. *et al.* Novel heterozygous NOTCH3 pathogenic variant found in two Chinese patients with CADASIL. *J Clin Neurosci* **46**, 85-89, doi:10.1016/j.jocn.2017.08.029 (2017).
84 Felli, M. P. *et al.* Expression pattern of notch1, 2 and 3 and Jagged1 and 2 in lymphoid and stromal thymus components: distinct ligand-receptor interactions in intrathymic T cell development. *Int Immunol* **11**, 1017-1025 (1999).
85 Austin, C. A. *et al.* TOP2B: The First Thirty Years. *Int J Mol Sci* **19**, doi:10.3390/ijms19092765 (2018).
86 Smith, K. A., Cowell, I. G., Zhang, Y., Sondka, Z. & Austin, C. A. The role of topoisomerase II beta on breakage and proximity of RUNX1 to partner alleles RUNX1T1 and EVI1. *Genes Chromosomes Cancer* **53**, 117-128, doi:10.1002/gcc.22124 (2014).
87 Cowell, I. G. & Austin, C. A. Do transcription factories and TOP2B provide a recipe for chromosome translocations in therapy-related leukemia? *Cell Cycle* **11**, 3143-3144, doi:10.4161/cc.21477 (2012).
88 Nebral, K., Schmidt, H. H., Haas, O. A. & Strehl, S. NUP98 is fused to topoisomerase (DNA) IIbeta 180 kDa (TOP2B) in a patient with acute myeloid leukemia with a new t(3;11)(p24;p15). *Clin Cancer Res* **11**, 6489-6494, doi:10.1158/1078-0432.CCR-05-0150 (2005).
89 Song, J. H. *et al.* High TOP2B/TOP2A expression ratio at diagnosis correlates with favourable outcome for standard chemotherapy in acute myeloid leukaemia. *Br J Cancer* **107**, 108-115, doi:10.1038/bjc.2012.206 (2012).

90 Beste, C., Stock, A. K., Epplen, J. T. & Arning, L. On the relevance of the NPY2-receptor variation for modes of action cascading processes. *Neuroimage* **102 Pt 2**, 558-564, doi:10.1016/j.neuroimage.2014.08.026 (2014).
91 Arning, L., Stock, A. K., Kloster, E., Epplen, J. T. & Beste, C. NPY2-receptor variation modulates iconic memory processes. *Eur Neuropsychopharmacol* **24**, 1298-1302, doi:10.1016/j.euroneuro.2014.03.003 (2014).
92 Benjamini, Y., and Hochberg, Y. . Controlling the false discovery rate: a practical and powerful approach to multiple testing. *Journal of the Royal Statistical Society Series B* **57**, 289-300 (1995).
93 Adzhubei, I. A. *et al.* A method and server for predicting damaging missense mutations. *Nat Methods* **7**, 248-249, doi:10.1038/nmeth0410-248 (2010).

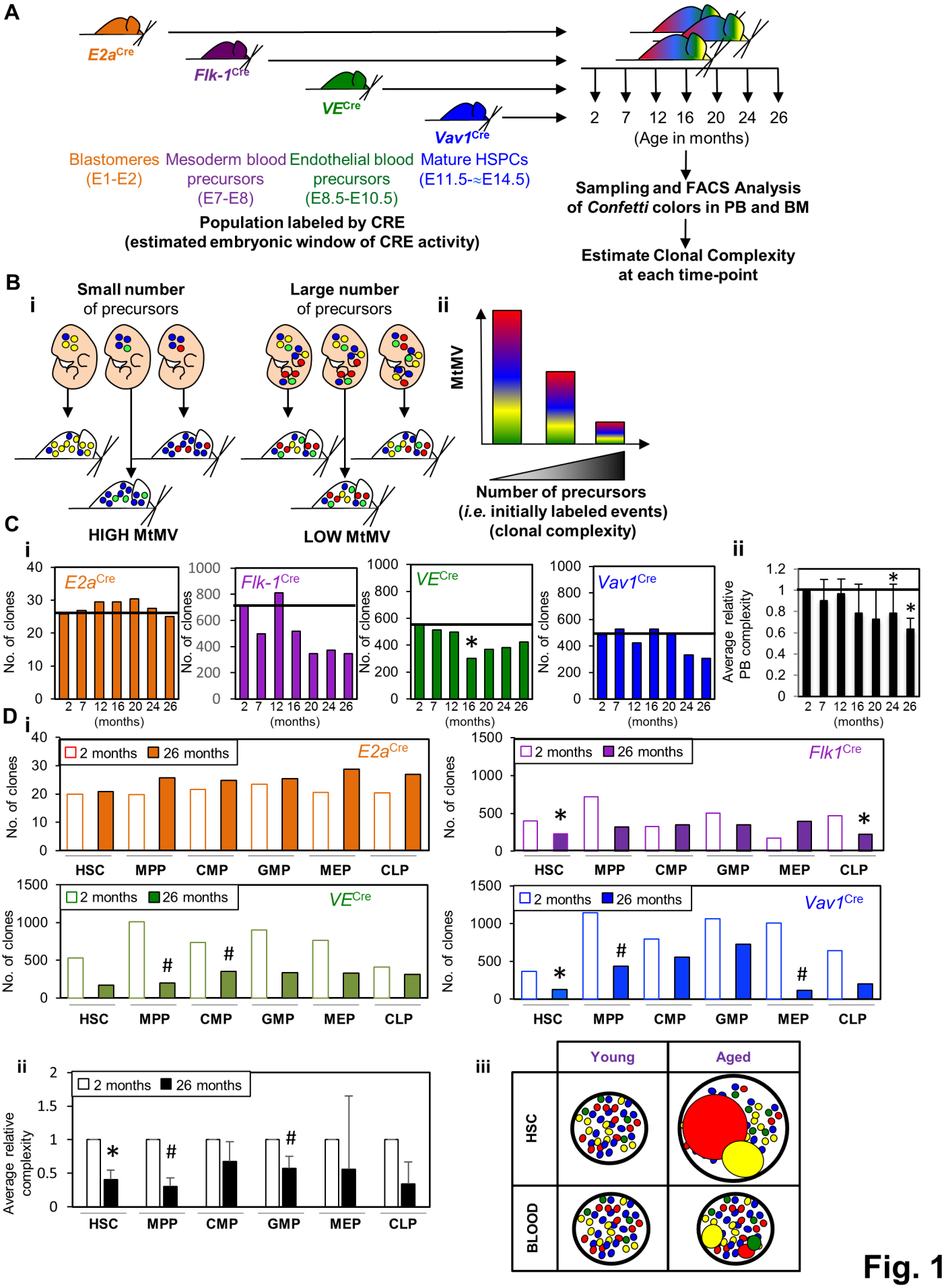
A
E2aCre
Flk-1Cre
VECre
Vav1Cre
2 7 12 16 20 24 26
(Age in months)
Blastomeres (E1-E2)
Mesoderm blood precursors (E7-E8)
Endothelial blood precursors (E8.5-E10.5)
Mature HSPCs (E11.5-≈E14.5)
Population labeled by CRE (estimated embryonic window of CRE activity)
Sampling and FACS Analysis of Confetti colors in PB and BM
Estimate Clonal Complexity at each time-point
B
i
Small number of precursors
Large number of precursors
HIGH MtMV
LOW MtMV
ii
MtMV
Number of precursors (i.e. initially labeled events) (clonal complexity)
C
i
No. of clones
(months)
ii
Average relative PB complexity
D
i
2 months
26 months
HSC MPP CMP GMP MEP CLP
ii
Average relative complexity
iii
Young
Aged
HSC
BLOOD

Fig. 1

A

Age in months		2	7	12	16	20	24	26
***Conf-E2a*^{Cre}**	Mouse 1							
	Mouse 2							
	Mouse 3							
***Conf-Flk-1*^{Cre}**	Mouse 1							
	Mouse 2							
	Mouse 3							
***Conf-VE*^{Cre}**	Mouse 1							
	Mouse 2							
	Mouse 3							
***Conf-Vav1*^{Cre}**	Mouse 1							
	Mouse 2							
	Mouse 3							

B

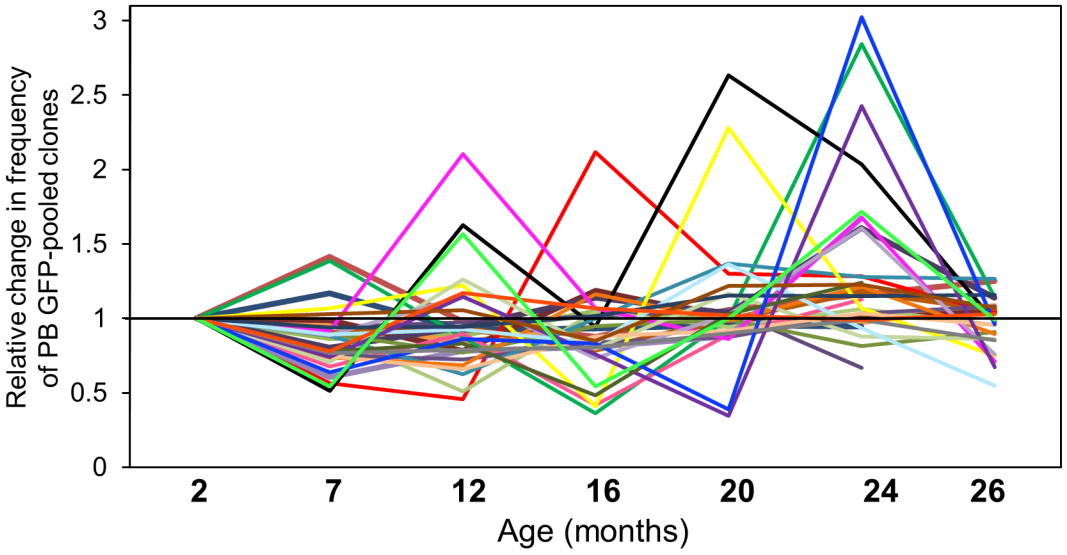

Figure 2

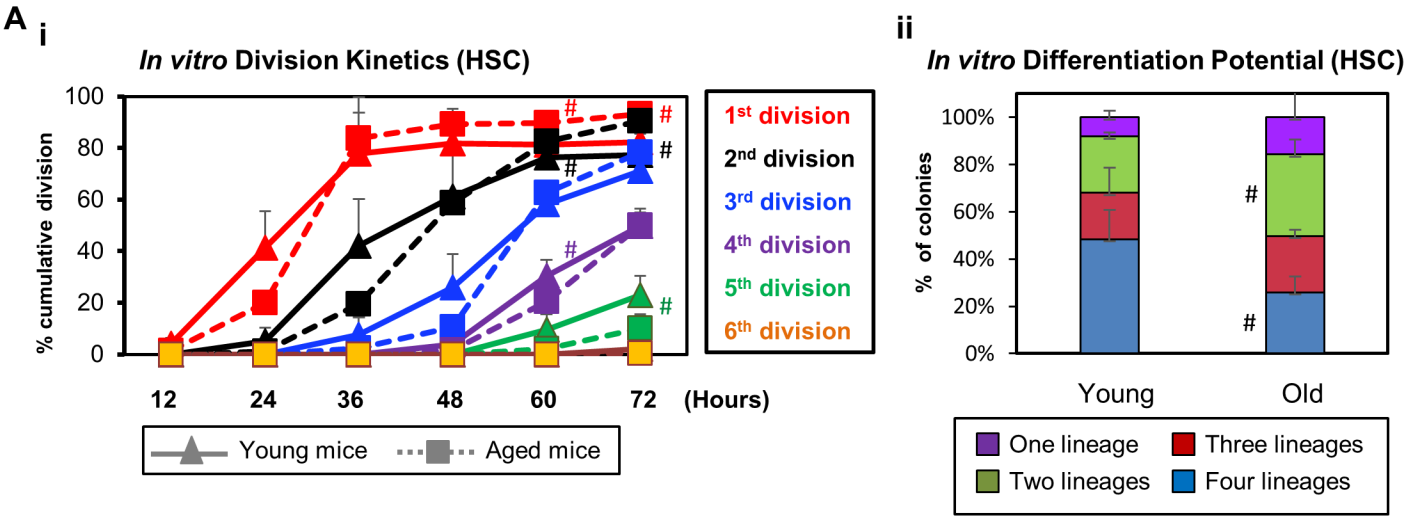

B

Mouse strain	ID	2 months of age						ID	26 months of age						
		HSC	MPP	CMP	GMP	MEP	CLP		PB	HSC	MPP	CMP	GMP	MEP	CLP
Conf-E2a^{Cre}	#1							#4							
	#2							#5							
	#3							#6							
Conf-Flk-1^{Cre}	#1							#4							
	#2							#5							
	#3							#6							
Conf-VE^{Cre}	#1							#4							
	#2							#5							
	#3							#6							
Conf-Vav1^{Cre}	#1							#4							
	#2							#5							
	#3							#6							

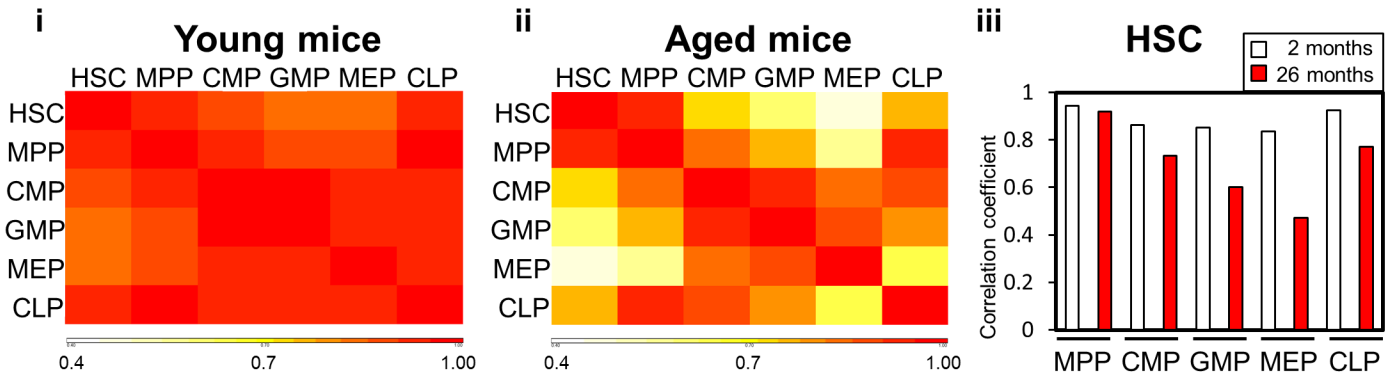

Figure 3

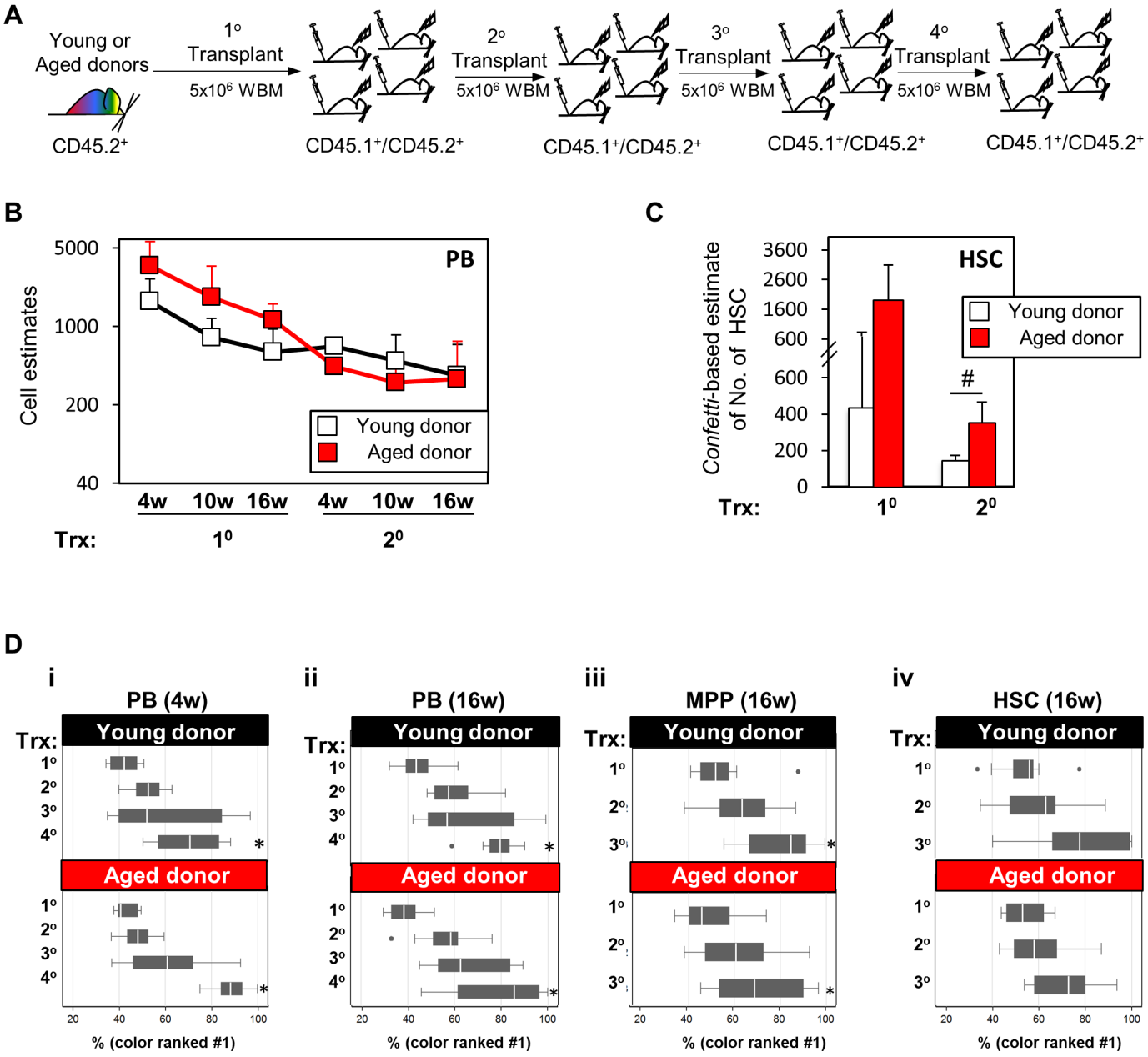
A
Young or Aged donors
CD45.2+
1° Transplant
5x10^6 WBM
CD45.1+/CD45.2+
2° Transplant
5x10^6 WBM
CD45.1+/CD45.2+
3° Transplant
5x10^6 WBM
CD45.1+/CD45.2+
4° Transplant
5x10^6 WBM
CD45.1+/CD45.2+
B
PB
Cell estimates
5000
1000
200
40
Young donor
Aged donor
4w 10w 16w 4w 10w 16w
Trx: 1⁰ 2⁰
C
HSC
Confetti-based estimate of No. of HSC
3600
2600
1600
600
600
400
200
0
#
Young donor
Aged donor
Trx: 1⁰ 2⁰
D
i
PB (4w)
ii
PB (16w)
iii
MPP (16w)
iv
HSC (16w)
Trx:
Young donor
Aged donor
1°
2°
3°
4°
*
20 40 60 80 100
% (color ranked #1)

Figure 4

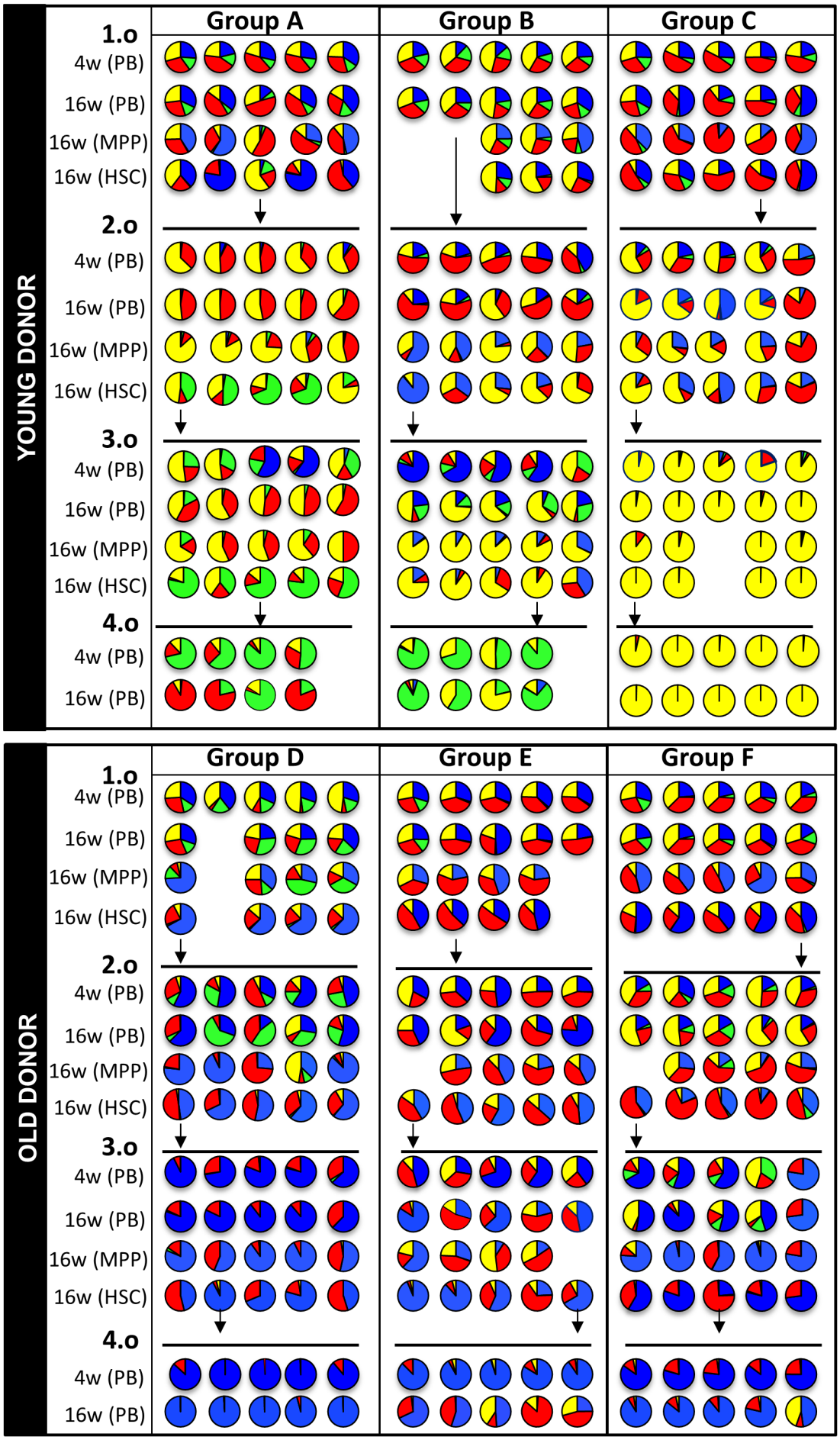
YOUNG DONOR
Group A
Group B
Group C
1.o
4w (PB)
16w (PB)
16w (MPP)
16w (HSC)
2.o
4w (PB)
16w (PB)
16w (MPP)
16w (HSC)
3.o
4w (PB)
16w (PB)
16w (MPP)
16w (HSC)
4.o
4w (PB)
16w (PB)
OLD DONOR
Group D
Group E
Group F
1.o
4w (PB)
16w (PB)
16w (MPP)
16w (HSC)
2.o
4w (PB)
16w (PB)
16w (MPP)
16w (HSC)
3.o
4w (PB)
16w (PB)
16w (MPP)
16w (HSC)
4.o
4w (PB)
16w (PB)

Figure 5

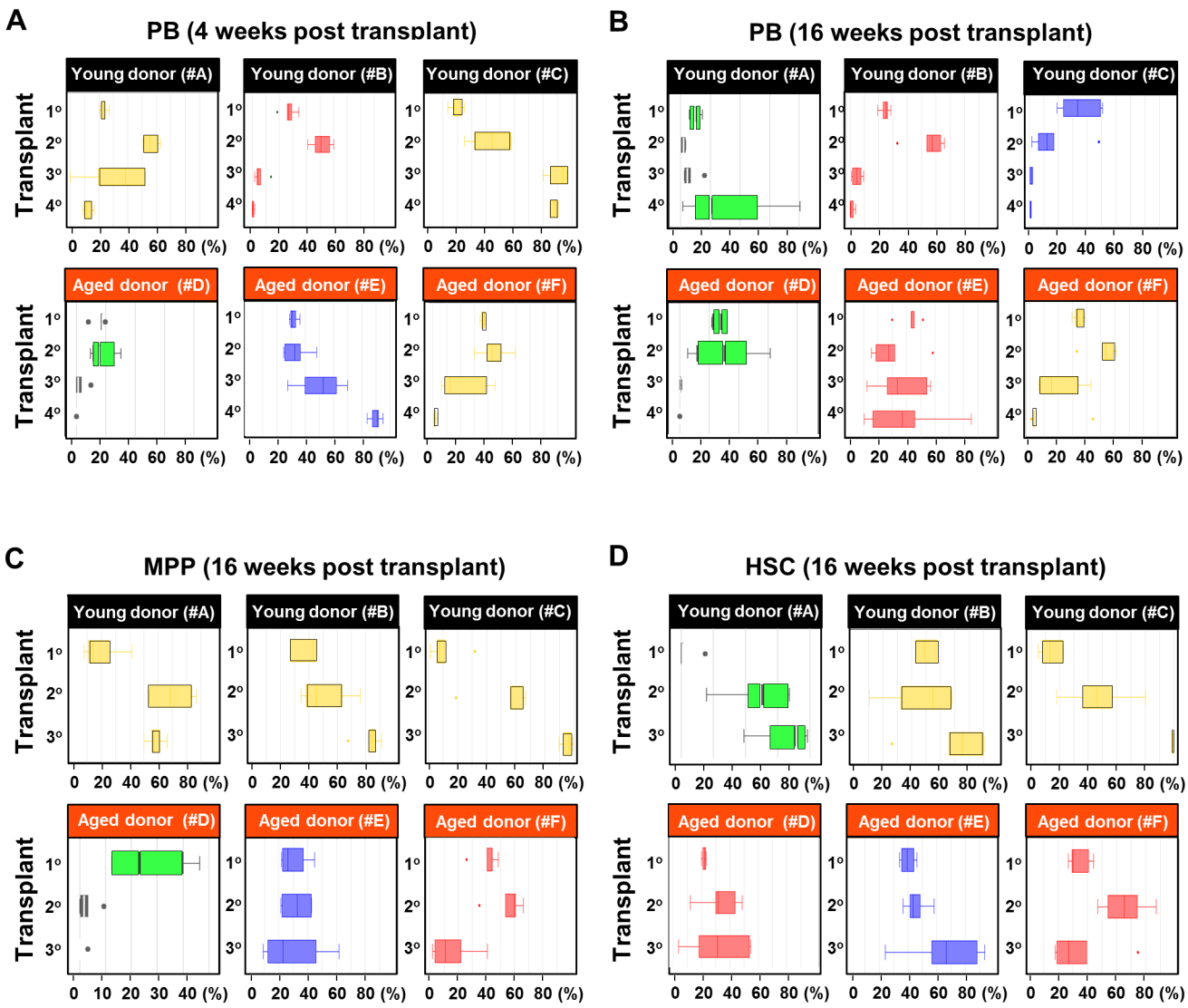
A
PB (4 weeks post transplant)
B
PB (16 weeks post transplant)
C
MPP (16 weeks post transplant)
D
HSC (16 weeks post transplant)
Young donor (#A)
Young donor (#B)
Young donor (#C)
Aged donor (#D)
Aged donor (#E)
Aged donor (#F)
Transplant
1º
2º
3º
4º
0 20 40 60 80 (%)
0 10 20 30 40 (%)

Figure 6

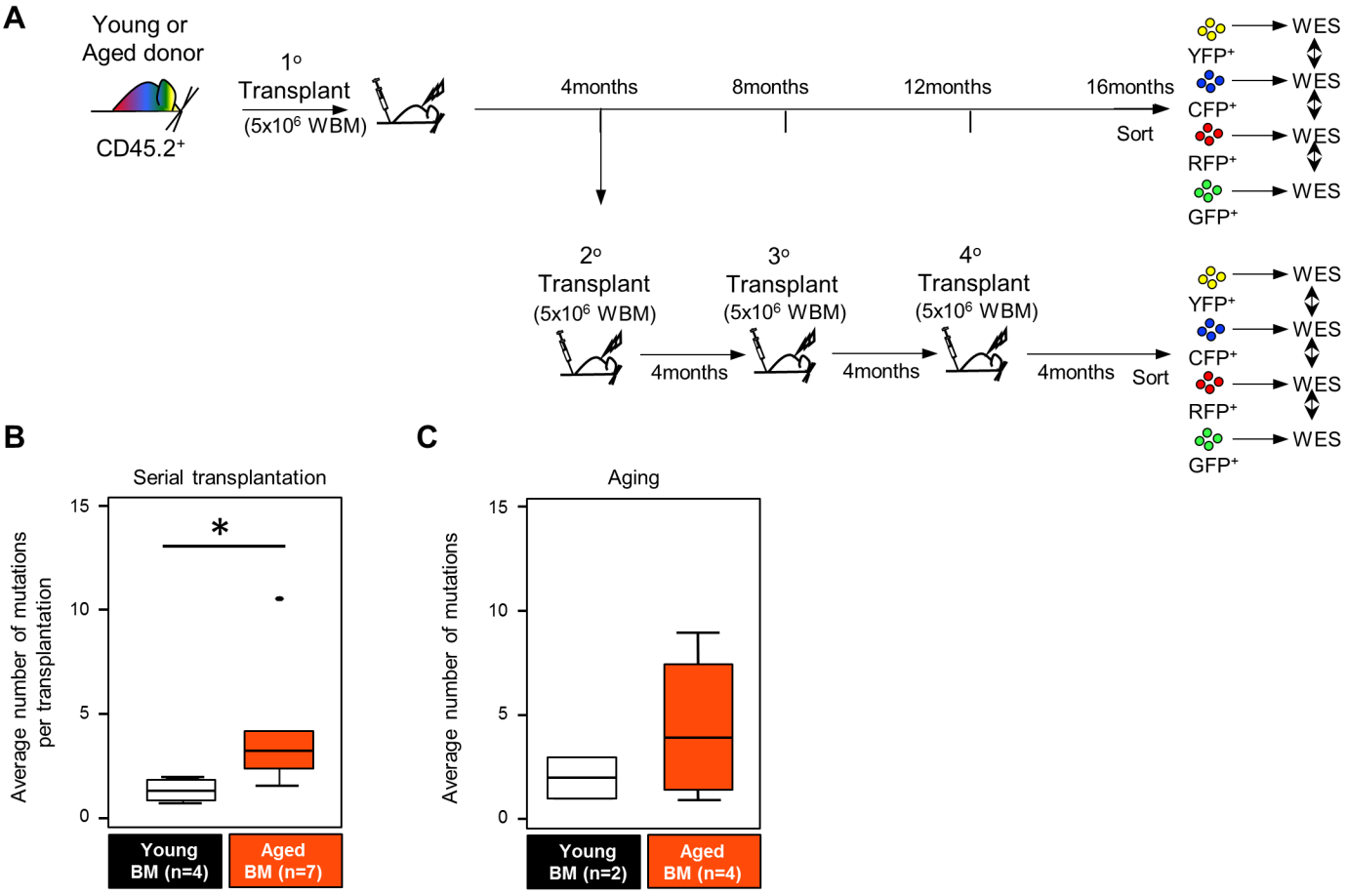
A
Young or
Aged donor
CD45.2+
1°
Transplant
(5x10^6 WBM)
4months
8months
12months
16months
Sort
YFP+
CFP+
RFP+
GFP+
WES
2°
Transplant
(5x10^6 WBM)
3°
Transplant
(5x10^6 WBM)
4°
Transplant
(5x10^6 WBM)
4months
4months
4months
Sort
B
Serial transplantation
Average number of mutations
per transplantation
15
10
5
0
*
Young
BM (n=4)
Aged
BM (n=7)
C
Aging
Average number of mutations
15
10
5
0
Young
BM (n=2)
Aged
BM (n=4)

Figure 7